



OPEN ACCESS

EDITED BY

Andrej Spiridonov,
Vilnius University, Lithuania

REVIEWED BY

Jacek Raddatz,
Helmholtz Association of German Research
Centres (HZ), Germany
Miriam Cobiانchi,
University of Pavia, Italy
Consuelo Sendino,
Natural History Museum, United Kingdom

*CORRESPONDENCE

David De Vleeschouwer,
✉ ddevlees@uni-muenster.de

RECEIVED 14 November 2024

ACCEPTED 08 April 2025

PUBLISHED 29 April 2025

CITATION

Lyu J, Barragán-Montilla S, Auer G, Bialik OM,
Del Gaudio AV, Sarr A-C and De
Vleeschouwer D (2025) Oxygenated bottom
water conditions on Broken Ridge (central
Indian Ocean) in the last 9 million years.
Front. Earth Sci. 13:1528487.
doi: 10.3389/feart.2025.1528487

COPYRIGHT

© 2025 Lyu, Barragán-Montilla, Auer, Bialik,
Del Gaudio, Sarr and De Vleeschouwer. This is
an open-access article distributed under the
terms of the [Creative Commons Attribution
License \(CC BY\)](https://creativecommons.org/licenses/by/4.0/). The use, distribution or
reproduction in other forums is permitted,
provided the original author(s) and the
copyright owner(s) are credited and that the
original publication in this journal is cited, in
accordance with accepted academic practice.
No use, distribution or reproduction is
permitted which does not comply with
these terms.

Oxygenated bottom water conditions on Broken Ridge (central Indian Ocean) in the last 9 million years

Jing Lyu¹, Sofía Barragán-Montilla^{2,3}, Gerald Auer⁴, Or M. Bialik¹, Arianna V. Del Gaudio¹, Anta-Clarisse Sarr⁵ and David De Vleeschouwer^{1*}

¹Institute of Geology and Paleontology, University of Münster, Münster, Germany, ²MARUM—Center for Marine Environmental Sciences, University of Bremen, Bremen, Germany, ³Institute of Geosciences, Kiel University, Kiel, Germany, ⁴University of Graz, Department of Earth Sciences (Geology and Paleontology), NAWI Graz Geocenter, Graz, Austria, ⁵University Grenoble Alpes, University Savoie Mont Blanc, Centre National de la Recherche Scientifique (CNRS), Institut de Recherche pour le Développement (IRD), University Gustave Eiffel, ISTerre, Grenoble, France

The Late Miocene and Early Pliocene were characterized by widespread oxygen depletion in the Pacific and Indian Oceans, coinciding with the “Late Miocene–Early Pliocene Biogenic Bloom” (LMBB). In the Indian Ocean, this oxygen depletion has been linked to enhanced productivity in the northern basins, leading to Oxygen Minimum Zone (OMZ) expansion. A longstanding hypothesis proposes that the OMZ extended south of Broken Ridge (~31°S). We test this hypothesis using benthic foraminiferal assemblages from ODP Site 752 (~1086 m water depth) spanning the last 9 Myr. We apply a semi-quantitative reconstruction of bottom water oxygenation using the Enhanced Benthic Foraminiferal Oxygen Index (EBFOI), benchmarked against the present-day core-top assemblage. Our results indicate persistently oxic bottom water conditions (3.2–5.2 mL/L) throughout the study interval. Although significant faunal changes occur, particularly between 5.5 and 2.2 Ma, these do not align with LMBB timing. Instead, we interpret assemblage shifts as responses to the intensification of Tasman Leakage, which brought oxygen-rich intermediate waters into the southern Indian Ocean. Our results challenge previous interpretations of OMZ expansion to Broken Ridge and highlight the role of southward water mass sourcing in shaping intermediate-depth oxygenation. This study provides a new mechanistic framework and emphasizes the importance of integrating faunal, sedimentological, and geochemical data to reassess regional OMZ histories.

KEYWORDS

OMZ expansion, biogenic bloom, benthic foraminifera, Indian Ocean, Broken Ridge, Tasman Leakage

1 Introduction

Oxygen minimum zones (OMZs) are regions in the ocean where oxygen saturation is at its lowest, typically found at depths below the mixing layer. These zones are crucial for understanding marine ecosystems as they represent the limit of survival for

aerobic marine organisms (Slater and Kroopnick, 1984). OMZs are formed in areas of high organic matter remineralization and play a significant role in the cycling of nutrients like phosphate, manganese, and iron (Lewis and Luther III, 2000; Kraal et al., 2012). Currently, the Indian Ocean hosts the thickest OMZ, which originates from the Arabian Sea upwelling zone and extends laterally up to 5,000 km into the central Indian Ocean, with a depth range between 200 and 2000 m (Wyrki et al., 1971; Jensen et al., 2011). The distribution of dissolved oxygen in the oceans is controlled by the balance between water mass ventilation and the remineralization of organic matter. During the Late Miocene to Early Pliocene, a significant oceanographic event known as the “Late Miocene Early Pliocene Biogenic Bloom” (LMBB) occurred, characterized by widespread oxygen depletion in the Pacific and Indian Oceans. This event is believed to have lasted for approximately 5 million years, from 9.0 Ma to 3.5 Ma (Dickens and Owen, 1994; Dickens and Owen, 1999; Hermoyian and Owen, 2001), and was associated with increased productivity in the northern basins of the Indian Ocean, leading to the expansion of the OMZ (Bialik et al., 2020; Auer et al., 2023).

A long-standing hypothesis suggests that the OMZ extended as far south as Broken Ridge (31°S) during the LMBB. This hypothesis is supported by two main lines of evidence: a depletion in manganese and the Mn/Sc ratio in Broken Ridge sediments between 6.5 and 3 Ma (Dickens and Owen, 1994), and a coeval drop in benthic foraminifera (BF) diversity along with an increase in the relative abundance of *Bolivina pusilla* and *Ehrenbergina carinata*, which are considered indicators of low-oxygen and high-productivity conditions (Singh et al., 2012; Gupta et al., 2013). However, these species are not exclusive to low-oxygen environments and can also be found under oxic conditions (Geslin et al., 2004). Furthermore, some benthic foraminifera are capable of surviving low-oxygen conditions via denitrification or kleptoplasty, introducing uncertainty into strict species-level oxygen classifications (Glock, 2023).

Late Miocene ocean-atmosphere simulations further support the southward expansion of the OMZ, showing a latitudinal range of oxygen-depleted intermediate waters comparable to the pre-industrial control simulation (Sarr et al., 2022) (Figure 1). However, these simulations assumed a pre-industrial global nutrient supply, which may underestimate the extent of Late Miocene oxygen depletion, as it is generally accepted that surface-ocean nutrient levels were globally higher during this period (Diester-Haass et al., 2002; Auer et al., 2023).

Nevertheless, the hypothesis of OMZ expansion remains a topic of debate. High-resolution productivity reconstructions based on XRF core scanning at ODP Site 752, developed and calibrated against organic carbon content in Lyu et al. (2023), do not indicate a significant productivity increase during the LMBB. This suggests that Broken Ridge has been in a nutrient-poor region of the South Indian gyre since the Middle Miocene. Additionally, sedimentological evidence indicates substantial winnowing at Site 752 during the LMBB (House et al., 1991; Lyu et al., 2023), which could explain the observed decrease in Mn and Mn/Sc ratios through diagenetic changes rather than a reduction in oxygen levels.

To further investigate the potential southward expansion of the Indian Ocean OMZ during the LMBB, we employed a multi-proxy approach focusing on benthic foraminiferal taxonomic

and quantitative analyses. Given that winnowing can affect geochemical proxies, our study uses benthic foraminifera to reconstruct changes in bottom-water oxygen concentrations over the past 9 Myr. We use the Enhanced Benthic Foraminiferal Oxygen Index (EBFOI) (Kranter et al., 2022), which allows semi-quantitative reconstruction of dissolved oxygen conditions based on full assemblage data. The EBFOI of the core-top assemblage at Site 752 aligns with today’s well-oxygenated waters (~4.5–5.0 mL/L), providing a robust benchmark for comparison.

Our reconstructions suggest persistent oxic conditions at Broken Ridge throughout the study interval, challenging the notion of a southward OMZ expansion to Broken Ridge during the LMBB. Instead, we propose that the observed shifts in benthic foraminiferal assemblages are more likely related to variations in the intensity of Tasman Leakage, which influences the characteristics of intermediate waters in the central southern Indian Ocean.

2 Materials and methods

2.1 Site description

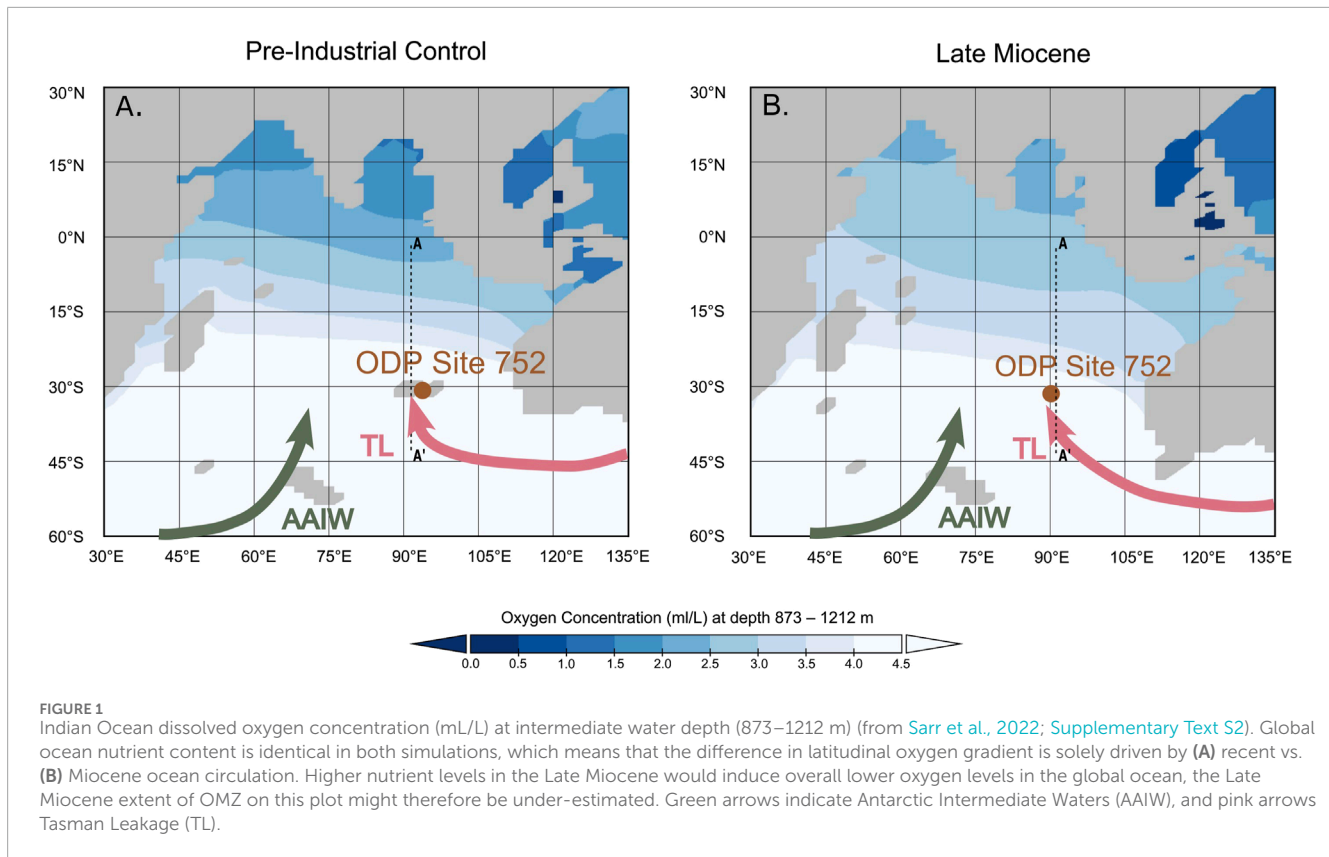
Ocean Drilling Program (ODP) Site 752 is located near the crest of Broken Ridge in the central Indian Ocean (30°53.475S, 93°34.652'E, present-day water depth of 1086.3 m, Figure 1A). Broken Ridge is a prominent bathymetric high that separated from the Kerguelen Plateau due to lithospheric extension and seafloor spreading that began before 42 Ma (Mutter and Cande, 1983; Berggren et al., 1985). As part of the Indo-Australian plate, Broken Ridge has moved northward by about 20 degrees of latitude since the Middle Eocene.

The sedimentary sequence at Site 752 consists predominantly of nannofossil and foraminiferal ooze with foraminiferal sand, with a calcium carbonate content ranging from 90.8% to 97.5%. This site has been located in intermediate water depths throughout the studied interval, providing a continuous record of sedimentation (Peirce et al., 1989; Driscoll et al., 1991).

2.2 Sample preparation

For this study, we used sediment samples from ODP Hole 752A, which were collected using the advanced hydraulic piston corer (APC). The samples span the last 9 Myr, based on the astrochronologic age-depth model proposed by Lyu et al. (2023). A total of 19 samples were selected from the interval between cores 752A-1H and 752A-4H (0–32.68 mbsf), with an average age resolution of 0.4 Myr between 9.1 and 2.2 Ma, allowing for detailed analysis of benthic ecological variability across the LMBB. The youngest sample was taken at 0.1 Ma to control the benthic foraminifera assemblage and estimate parameters in modern times.

Each sample (~2 cm thick) was processed to remove the fine fraction (<63 μm), dried, and dry-sieved. The 63–350 μm fraction was dry-split using a micro-splitter, and benthic foraminifera were picked, sorted, and identified under a binocular microscope. Preservation was generally good, with specimens largely intact (Figure 2). Genus determinations were based on Loeblich Jr and Tappan (2015), and specific identifications follow mainly from



Bolli et al. (1994), Holbourn et al. (2013), and Van Morkhoven (1986), among others. An average of 348 specimens per sample (range: 245–498) were identified, yielding a total of 93 benthic foraminifera species (Supplementary Text S1; Figure 3).

2.3 Benthic foraminiferal analysis

The analysis of benthic foraminifera was conducted to determine the diversity and reconstruct the dissolved oxygen concentration at the seafloor. The raw counts of benthic foraminifera relative frequencies (Supplementary Table S1) were used to calculate the Fisher Alpha diversity index (Fisher et al., 1943).

Additionally, the Enhanced Benthic Foraminifera Oxygen Index (EBFOI) was employed to estimate the dissolved oxygen concentration, following the method described by Kranner et al. (2022). This approach offers a comprehensive update to the Benthic Foraminifera Oxygen Index (BFOI) originally proposed by Kaiho (1994). The EBFOI is derived from the relative abundances of species classified as oxic, suboxic, or dysoxic. The index was calibrated using globally distributed modern datasets (Kranner et al., 2022), yet it was not specifically tailored to conditions at Broken Ridge. However, more than 99% of the specimens identified in the Site 752 samples could be categorized using established classification schemes (Supplementary Table S1), giving a clear picture of past ecology changes at Broken Ridge. Nevertheless, we recognize the inherent uncertainties in assigning extinct taxa and the absence of local calibration. Consequently, we interpret the EBFOI as a semi-quantitative proxy, appropriate for tracking relative changes

in bottom water oxygenation rather than providing absolute values of dissolved oxygen.

A full assemblage assessment was performed, which allows for more reliable estimations compared to the presence/abundance of individual species. All identified species were classified according to their microhabitat (infaunal or epifaunal) (Jorissen et al., 1995), whether they are considered stress species (van der Zwaan et al., 1990; Kouwenhoven, 2000), and their oxygen-level preference (oxic, suboxic, or dysoxic; Supplementary Table S1). To retain a robust signal of benthic foraminifera distribution without single and scattered occurrences, taxa with abundances below 5% across all samples were removed before the cluster analysis (Supplementary Table S3).

The following groupings were needed to ensure robust signals of benthic foraminifera distribution without single and scattered occurrences.

- *Cibicidoides* sp. and *Cibicidoides* sp.1 were combined into *Cibicidoides* spp.
- *Chrysalogonium equisetiformis* (only one specimen) was grouped with *Chrysalogonium deceptorium*
- *Quinqueloculina* sp. was combined with *Quinqueloculina seminula*
- *Favulina hexagona* and *F. squamosa* were counted together as *Favulina hexagona/squamosa*
- *Melonis barleeanus* and *Melonis* sp. were grouped as *Melonis barleeanus*
- *Pullenia bulloides* and *Pullenia quinqueloba* were combined into *Pullenia bulloides/quinqueloba*

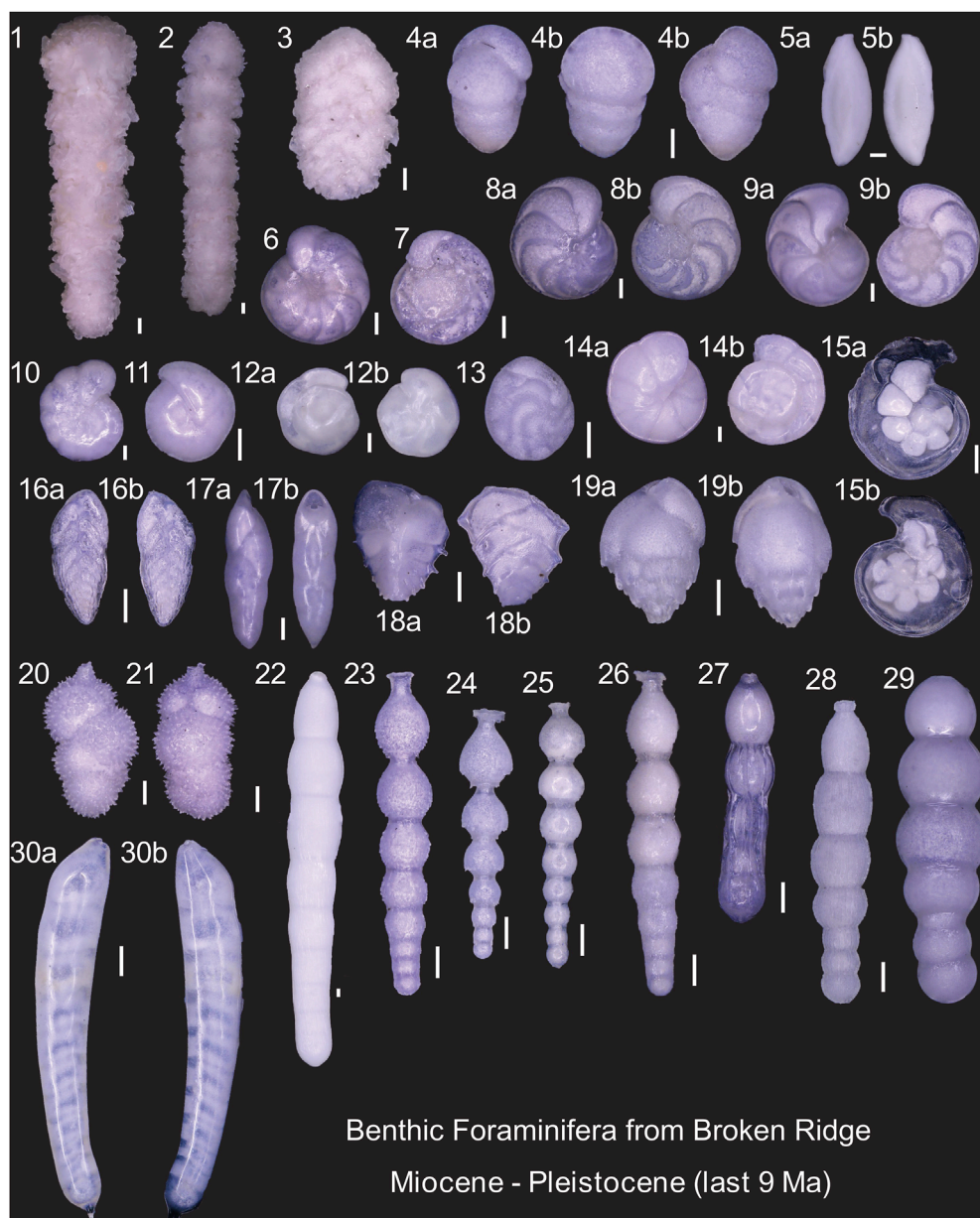


FIGURE 2

Benthic foraminifera at Broken Ridge from the Late Miocene to recent shows good preservation. 1. *Clavulina* sp.1 (sample from ODP 121–752A, 3H-4, 52–54 cm); 2. *Clavulina* sp.1 (3H-5, 124–126); 3. *Spiroplectinella* sp. (2H-3, 118–120); 4. *Eggerella bradyi* (2H-4, 118–120); 5. *Spirosigmoilina tenuis* (3H-3, 10–12); 6. *Cibicidoides mundulus* (2H-2, 100–102) ventral side; 7. *Cibicidoides mundulus* (2H-3, 118–120); dorsal side; 8. *Cibicidoides wuellerstorfi* (3H-4, 52–54); a. Ventral side, b. Dorsal side; 9. *Hanzawaia* cff. *Boueana* (3H-2, 82–84); a. Ventral side, b. Dorsal side; 10. *Anomalinoidea globulosus* (2H-CC, 4–6); 11. *Pullenia bulloides* (2H-1, 88–90); 12. *Oridorsalis umbonatus* (2H-1, 88–90); a. Ventral side, b. Dorsal side; 13. *Gyroidina soldanii* (1H-1, 34–36); a. Ventral side, b. Dorsal side; 15. *Laticarinina pauperata* (2H-2, 100–102); a. Ventral side, b. Dorsal side; 16. *Bulimina striata* (1H-5, 22–24); a. Ventral side, b. Dorsal side; 17. *Pleurostomella* sp.1; (2H-CC, 4–6); a. Frontal view, b. Side view; 18. *Ehrenbergina carinata* (3H-1, 118–120); a. Frontal side, b. Dorsal side; 19. *Bulimina striata* (1H-5, 22–24); a. Dorsal side, b. Frontal side; 20. *Siphonodosaria lepidula* (3H-4, 52–54); 21. *Siphonodosaria lepidula* (3H-4, 52–54); 22. *Chrysalogonium equisetiformis* (2H-2, 100–102); 23. *Siphonodosaria lepidula* (2H-1, 88–90); 24. *Siphonodosaria lepidula* (2H-2, 100–102); 25. *Siphonodosaria pomuligera* (2H-1, 4–6); 26. *Siphonodosaria pomuligera* (2H-1, 88–90); 27. *Orthomorphina* sp.; (2H-CC, 4–6) 28. *Glandulonodosaria ambigua* (2H-1, 4–6); 29. *Orthomorphina perversa* (3H-1, 10–12); 30. *Siphonodosaria consorbina* (2H-2, 100–102); a. Side view, b. Side view. All white scale bars represent 100 μ m.

- All *Fissurina* species were counted as *Fissurina* spp. due to identification difficulties
- *Lagena* spp. includes *Lagena hispida*, *L. nebulosi*, *L. striata*, and *Lagena* sp.

- *Lenticulina* spp. contains *Lenticulina calcar*, *L. cultrata*, and *Lenticulina* sp.1
- *Pluerostomella* spp. includes *P. acuminata*, *P. brevis*, and *Pluerostomella* sp.1

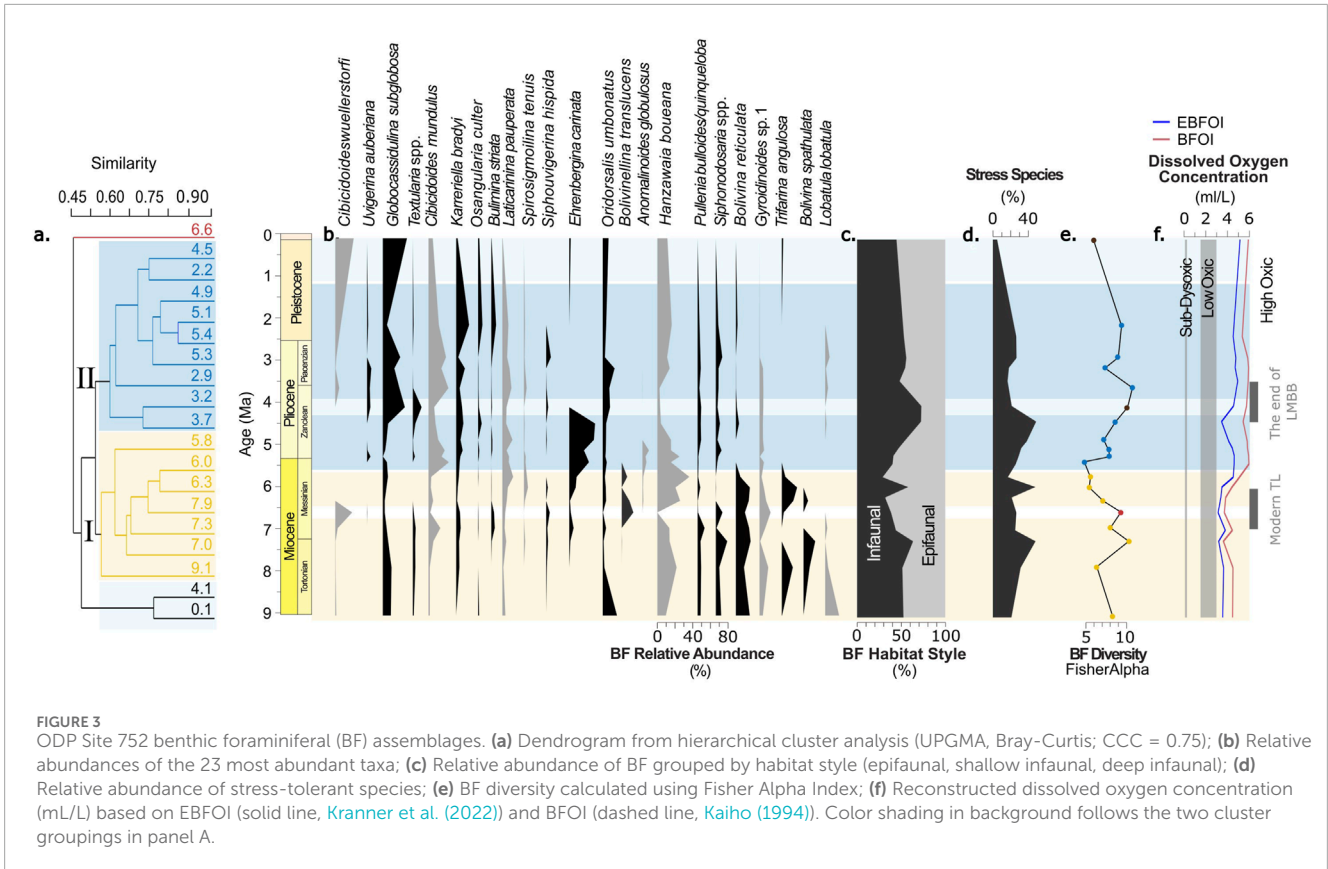


FIGURE 3 ODP Site 752 benthic foraminiferal (BF) assemblages. **(a)** Dendrogram from hierarchical cluster analysis (UPGMA, Bray-Curtis; CCC = 0.75); **(b)** Relative abundances of the 23 most abundant taxa; **(c)** Relative abundance of BF grouped by habitat style (epifaunal, shallow infaunal, deep infaunal); **(d)** Relative abundance of stress-tolerant species; **(e)** BF diversity calculated using Fisher Alpha Index; **(f)** Reconstructed dissolved oxygen concentration (mL/L) based on EBFOI (solid line, [Kranner et al. \(2022\)](#)) and BFOI (dashed line, [Kaiho \(1994\)](#)). Color shading in background follows the two cluster groupings in panel A.

- *Rectuvigerina* spp. comprises *Rectuvigerina cf. Phlegari*, *Rectuvigerina striata*, and *Rectuvigerina* sp.
- The *Siphonodosaria* species were grouped for analysis and interpretation due to sub-optimal preservation, containing *Siphonodosaria consorbina*, *S. hispidula*, *S. lepidula*, *S. pomuligera*, *Siphonodosaria* sp.1, *Siphonodosaria* sp.2, *Siphonodosaria* sp.4, *Siphonodosaria* sp.5, and *Siphonodosaria* spp.
- *Uvigerina* spp. includes *Uvigerina peregrina* and two species (*Uvigerina* sp.1 and *Uvigerina* sp.2) with similar morphology.

2.3.1 Dissolved oxygen reconstruction (BFOI and EBFOI)

To reconstruct the dissolved oxygen concentration at the seafloor, we utilized the Benthic Foraminifera Oxygen Index (BFOI) and the Enhanced Benthic Foraminifera Oxygen Index (EBFOI). These indices are particularly suitable for open ocean settings and relatively high oxygen conditions, allowing for a broader range of oxygen levels to be assessed compared to other indices.

The BFOI, as defined by [Kaiho \(1994\)](#), is calculated using the formula:

$$BFOI = 100 \left(\frac{O}{(O + D)} \right)$$

where (O) represents the number of oxic species and (D) represents the number of dysoxic species. The EBFOI,

described by [Kranner et al. \(2022\)](#), is calculated using the formula:

$$EBFOI = 100 \left(\frac{O}{O + D + \frac{S}{2}} \right)$$

where (S) represents the number of suboxic species. These formulas take into account the relative abundances of oxic, dysoxic, and suboxic species within the benthic foraminifera assemblages.

More than 99% of the specimens in our samples belonged to a species that has been classified according to their oxygen sensitivity (see classification in [Supplementary Table S1](#)). This classification is primarily based on the works of [Kaiho \(1994\)](#) and [Kranner et al. \(2022\)](#).

2.3.2 Cluster analysis

To identify patterns in the benthic foraminiferal assemblages, we performed a cluster analysis on the benthic foraminiferal abundances' dataset. Cluster analysis helps to group samples with similar species compositions, which can provide insights into the paleoenvironmental conditions at the time of deposition. Before conducting the cluster analysis, we filtered the benthic foraminiferal dataset to remove taxa with relative abundances lower than 5% across all samples. This step ensures that the analysis focuses on the most significant taxa, reducing noise from rare species. Supra-specific groups were used to combine low-abundance taxa, further decreasing the noise in the analysis. We used the Bray-Curtis distance as a measure of dissimilarity between samples, which is appropriate for ecological data ([Bray and Curtis, 1957](#)). The unweighted paired group with arithmetic mean (UPGMA)

method was chosen as the amalgamation algorithm for hierarchical clustering (Sokal, 1965). This method is also known as group average clustering. The cophenetic correlation coefficient (CCC) was calculated to assess the goodness of fit of the cluster analysis. The CCC measures the correlation between the original dissimilarities and the dissimilarities implied by the dendrogram (Sokal and Rohlf, 1962). Here, we obtained a CCC value of 0.75, indicating a good fit and suggesting that the dendrogram reasonably represents the dissimilarities in the data.

Cluster analysis was carried out using the PAST software package, version 4.12b (Hammer and Harper, 2001). This software provides a comprehensive set of tools for paleontological data analysis, including cluster analysis.

2.4 Mass accumulation rate

The carbonate mass accumulation rate (MAR) was calculated to estimate the flux of carbonate to the seafloor. MAR is expressed in $\text{g}/\text{cm}^2/\text{kyr}$ and was determined using the formula:

$$\text{MAR} = \text{wt}\% \times \text{SR} \times \text{DBD}$$

where wt% is CaCO_3 content, SR is sedimentation rate (cm/kyr), and DBD is dry bulk density (g/cm^3). SR values are based on the age model in Lyu et al. (2023), and CaCO_3 and DBD were obtained from shipboard measurements (Peirce et al., 1989).

3 Oxic conditions at Broken Ridge throughout the Miocene, Pliocene and Quaternary

The benthic foraminiferal (BF) assemblages from ODP Site 752 on Broken Ridge reveal dynamic but consistently moderate ecological conditions across the last 9 Myr (Figure 3). BF diversity, evaluated using the Fisher Alpha index, remains moderate (between 5 and 10) throughout the interval, with a notable dip near five at approximately 5.4 Ma (Figure 3e). Infaunal species composition fluctuates, peaking at 72.9% between 4.5 and 4.1 Ma, while stress-associated species remain relatively stable, never exceeding 48.8% (Figures 3c,d). These findings collectively suggest steady and moderate oxygenation levels throughout this time.

The absence of consistent trends or remarkable features in benthic foraminiferal species assemblage during the Late Miocene Biogenic Bloom (LMBB) aligns with the outcome of our cluster analysis (Figure 3a), which identifies two distinct assemblage groups not aligned with LMBB timings. Cluster I (9.1–5.8 Ma) is characterized by the dominance of *Hanzawaia boueana*, *Siphonodosaria* spp., *Bolivina spathulata*, and *Bolivina reticulata*, whereas *Cibicidoides wuellerstorfi*, *Ehrenbergina carinata*, and *Textularia* spp. remain scarce or absent. In contrast, Cluster II (5.5–2.2 Ma) exhibits increased occurrences of *Globocassidulina subglobosa*, *Cibicidoides mundulus*, *Oridorsalis umbonatus*, and *Uvigerina auberiana*, alongside reduced abundance of *Hanzawaia boueana* compared to Cluster I. These cluster-defined groups reflect an assemblage shift that does not coincide with the timing of the LMBB, suggesting that factors other than productivity variations

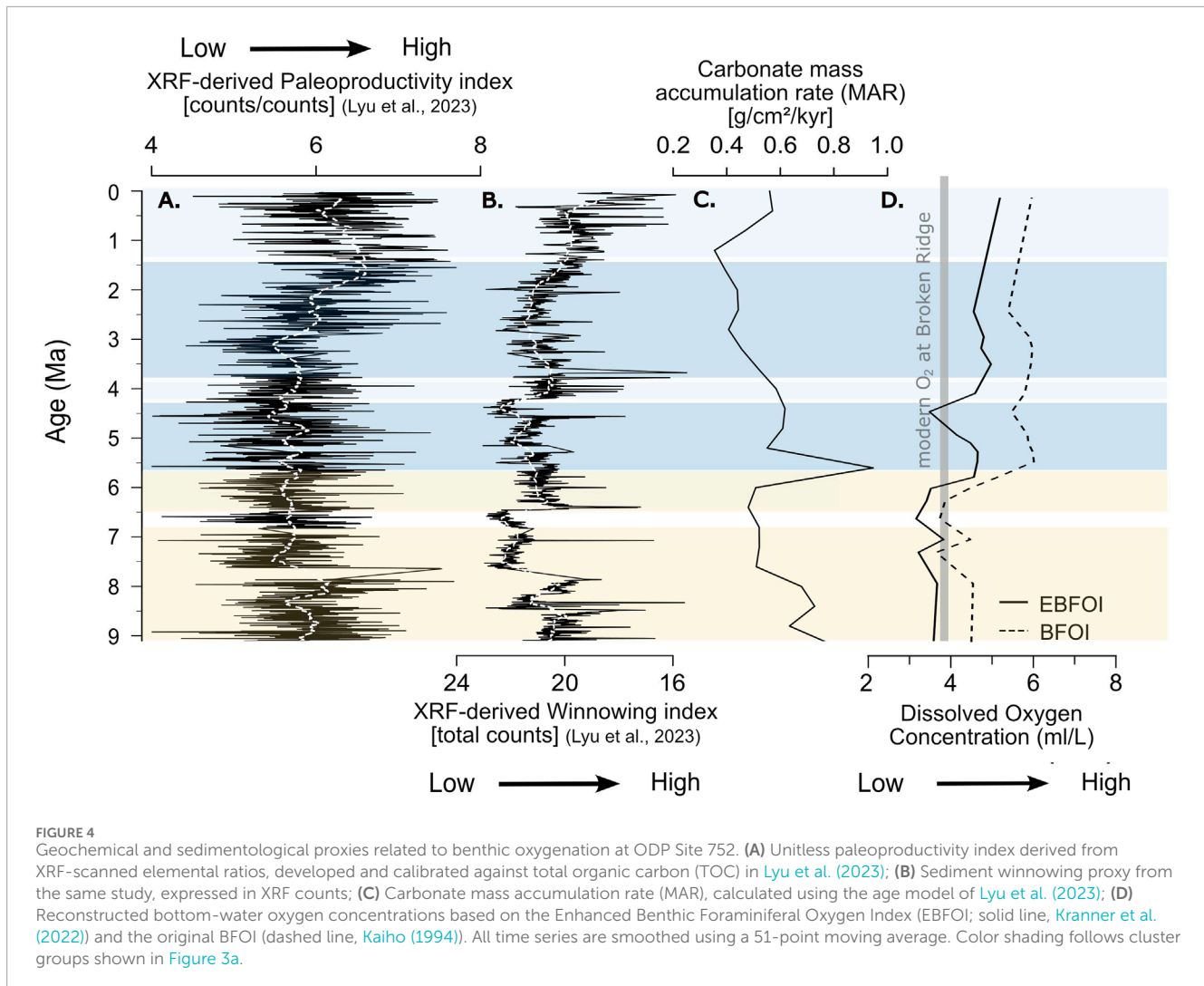
drove the observed ecological transitions. Ecologically, the shift between the two clusters represents a transition from a community dominated by species associated with relatively stable, low-nutrient environments toward one favoring taxa indicative of well-ventilated, oxic intermediate waters.

Oxygen levels reconstructed through Benthic Foraminifera Oxygen Index (BFOI) and Enhanced BFOI (EBFOI) indicate well-oxygenated bottom waters across the studied interval (Figures 3f, 4D). The average EBFOI-based oxygen concentration is 4.2 mL/L, comparable to modern levels on Broken Ridge and persistently above 3.2 mL/L, supporting a high-oxygen environment. The prominence of oxic species, such as *Cibicidoides wuellerstorfi* and *Globocassidulina subglobosa*, further substantiates this conclusion. However, we emphasize that the EBFOI should be considered here as a semi-quantitative proxy, useful for tracking relative oxygenation changes rather than absolute concentrations. This is because alternative metabolic strategies (e.g., denitrification, fermentation, kleptoplasty) among benthic foraminifera (Geslin et al., 2004) can decouple past species distributions from oxygen alone. Furthermore, agglutinated taxa are underrepresented in our assemblages due to preservation issues, potentially influencing EBFOI results in the lower oxygen range. Yet, we note that the EBFOI of the youngest sample (~0.1 Ma) closely aligns with present-day bottom water oxygenation (~4.5–5.0 mL/L), lending credibility to the entire record's internal consistency.

BF analyses thus underscore that Broken Ridge's intermediate waters retained oxic conditions throughout the Late Miocene to Early Pleistocene. We interpret this pattern as the result of sustained influence from southern-sourced, well-oxygenated water masses, likely Tasman Leakage or Antarctic Intermediate Water, rather than from local productivity changes or OMZ expansion. This finding challenges previous assumptions of OMZ expansion and its impact on Broken Ridge, though we emphasize that our interpretation represents a hypothesis grounded in foraminiferal ecology. In the following section, we assess whether sedimentological and geochemical records provide additional support for this interpretation.

4 Limits on OMZ expansion and the role of Tasman Leakage

Our findings indicate that the influence of the Late Miocene Biogenic Bloom (LMBB) on the southeastern Indian Ocean, especially at Broken Ridge, warrants re-evaluation. Dickens and Owen (1999) emphasized that understanding productivity changes in the central Indian Ocean during the LMBB is critical for assessing broader paleoceanographic impacts. Indeed, the central Indian Ocean is a dynamically complex region where multiple water masses converge and interact. During the Miocene–Pliocene transition, the intermediate water mass configuration of the Indian Ocean was shaped by the competing contributions of Antarctic Intermediate Water (AAIW), Indonesian Intermediate Waters (IIW), and Tasman Leakage (Christensen et al., 2021). Quaternary reconstructions of intermediate water dynamics (You, 2000; Piotrowski et al., 2009; Struve et al., 2022; Raddatz et al., 2023) highlight the role of remote sourcing and ventilation in controlling bottom water oxygenation



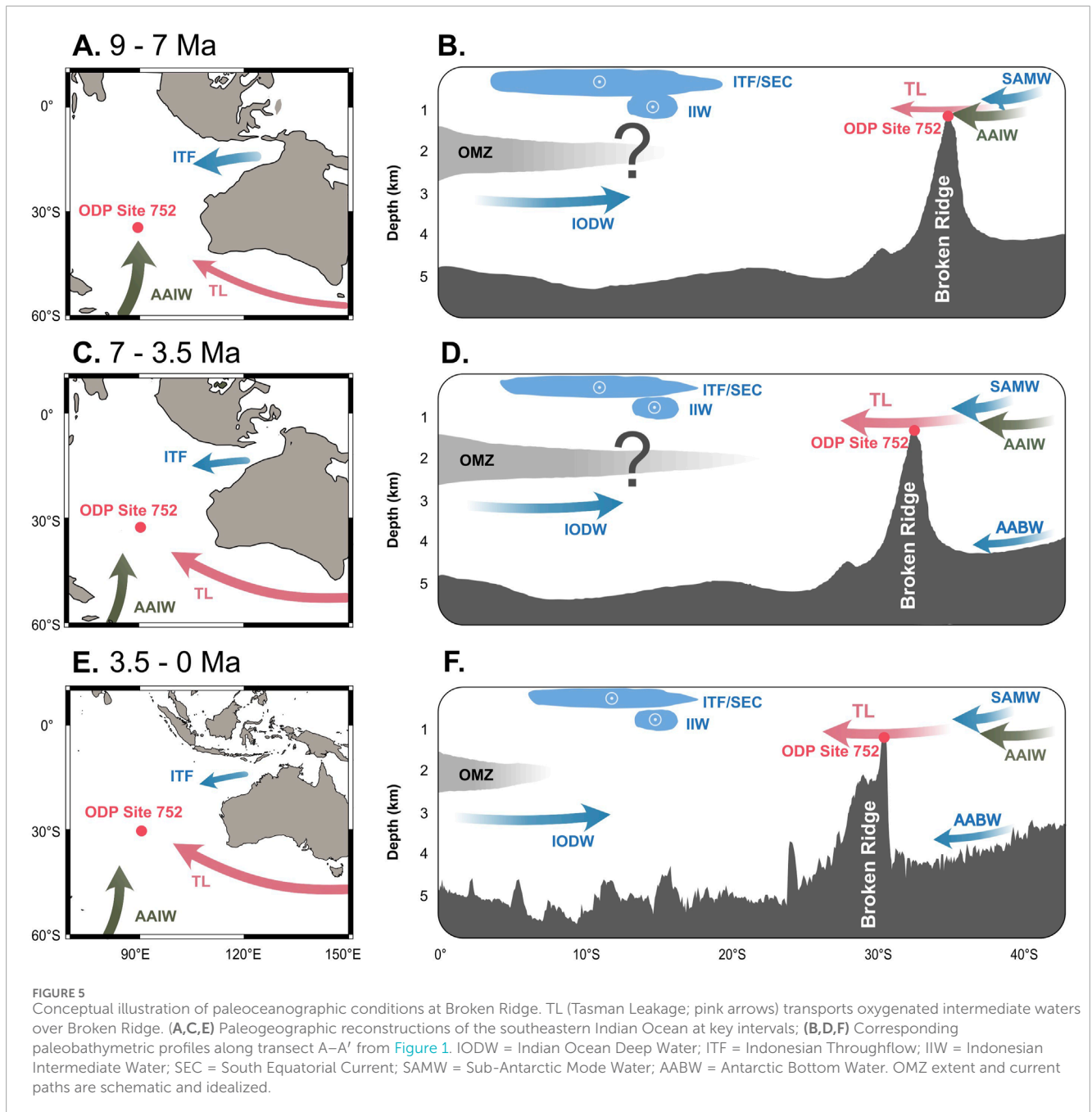
across the Indian Ocean—mechanisms that likely also extend to earlier intervals.

In previous work (Lyu et al., 2023), we presented an XRF-derived paleoproductivity proxy from Site 752 (also shown in Figure 4A), which demonstrated consistently low productivity levels during the LMBB. The XRF-derived productivity index was developed by utilizing a group of metallic micronutrients (Cd, Cu, Ni, Zn, Cr and Br) divided by Ca counts. This paleoproductivity index was calibrated against directly measured organic carbon contents from discrete samples at ODP Site 752 (Lyu et al., 2023). This proxy suggests that Broken Ridge likely remained an oligotrophic zone within the central South Indian gyre since the Late Miocene, positioned away from nutrient-rich waters at the subtropical front to the south and from continental nutrient sources to the north.

Previous benthic foraminifera assemblage studies at Broken Ridge, however, came to different conclusions. Indeed, studies by Singh et al. (2012) and Gupta et al. (2013) suggested that the OMZ extended southward to Broken Ridge, based on reduced BF diversity and increased low-oxygen taxa during the LMBB.

These low-oxygen indicators, including *Uvigerina peregrina* and *Trifarina angulosa*, correlate with oxygen depletion and heightened productivity. Although our assemblages also show the presence of these taxa in Late Miocene and Early Pliocene samples, their relatively low abundance—alongside a strong presence of oxic species—supports our alternative interpretation. The dominance of oxic species throughout this period suggests persistently well-oxygenated conditions, casting doubt on the OMZ expansion hypothesis at Broken Ridge (Figure 3f).

While our assemblage data diverge from previous interpretations in the above-described aspect, they are not entirely incompatible with Singh et al. (2012) and Gupta et al. (2013). Moreover, we highlight that our observations are consistent with the “little-faunal-turnover” conclusion by Ridha et al. (2019) for Neogene benthic foraminiferal assemblages at Broken Ridge. All Broken Ridge benthic assemblage studies, including ours, report increased low-oxygen, high-productivity taxa alongside higher stress and infaunal taxa abundances from 5.1 to 4.1 Ma (Figures 3c,d), indicating a minor decline in oxygen, but within overall oxic conditions. BF diversity, shown by the Fisher Alpha



index (Figure 3e), decreases slightly between 7.0 and 4.1 Ma, consistent with earlier studies. However, our cluster analysis (Figure 3a) does not align this trend with the LMBB period. Additionally, XRF-derived productivity proxies (Figure 4A) do not suggest a substantial LMBB effect at Site 752, likely due to the unique paleoceanographic configuration at Broken Ridge (Lyu et al., 2023; Pillot et al., 2023). Together, these findings imply that neither productivity increases nor oxygen depletion drove BF distributions on Broken Ridge across this interval.

Instead, we propose that the primary factor influencing BF variability at Site 752 was Pacific-sourced Tasman Leakage (TL) waters. XRF geochemical and grain-size analyses (Lyu et al., 2023;

Figure 4B) show an increase in winnowing from approximately 7 Ma, aligning with the onset of the modern TL circulation (Christensen et al., 2021). TL currents intensified between seven and 4 Ma, bringing low-nutrient, higher-oxygen waters to Broken Ridge and favoring oxic BF species. The peak winnowing effect, as indicated by grain-size and BF distribution data, occurs around 4 Ma, coinciding with increased *Cibicidoides wuellerstorfi*, shifts in stress species, and infaunal species composition (Figures 3b,c). *C. wuellerstorfi*'s epiphytic lifestyle suggests adaptation to stronger bottom currents introduced by TL (Linke and Lutze, 1993). The decrease in Mn and Mn/Sc, initially interpreted as indicative of decreasing oxygen levels according to (Dickens and Owen, 1999),

could instead be explained by a change in sediment composition due to winnowing, where finer, Mn-enriched particles are removed, while Sc remains relatively evenly distributed across the sediment fraction. This reinterpretation is supported by the sedimentological changes at Site 752 and does not require invoking redox-driven early diagenesis.

Further evidence to support TL's role in shaping Broken Ridge's oxygen levels comes from carbonate MARS. This proxy is commonly used to quantify productivity throughout the LMBB (Lyle et al., 2019; Karatsolis et al., 2022; Sutherland et al., 2022; Gastaldello et al., 2023). Carbonate MARS at Broken Ridge peak around 5.5 Ma (Figure 4C), yet show no sustained increase during the LMBB, reinforcing a generally low-productivity environment at Broken Ridge. The steady CaCO₃ content over this period suggests that MAR variability mainly reflects sedimentation rate changes rather than shifts in nutrient availability or organic matter deposition.

Our model, which highlights a strong TL influence dominating intermediate water conditions over Broken Ridge since the Late Miocene (Christensen et al., 2021; Lyu et al., 2023), provides a more compelling explanation for the high-oxygen conditions observed at Broken Ridge during the Late Miocene and Early Pliocene than a southward expansion of the OMZ. TL likely acted as a barrier to OMZ encroachment, maintaining a nutrient-poor, well-oxygenated environment over Broken Ridge throughout the LMBB and beyond. Arguably, this interpretation is solely based on indirect faunal and sedimentological evidence. Future work should include direct geochemical tracers (e.g., $\delta^{13}\text{C}_{\text{benthic}}$, $\epsilon\text{Nd}(t)$, Mg/Ca, clumped isotopes, total organic carbon, and total nitrogen) to robustly test the role of TL and water mass sourcing in maintaining oxic conditions at Broken Ridge. When confirmed, this mechanism underscores the role of TL as a key factor in controlling southeastern Indian Ocean oxygenation patterns at intermediate depths (Figure 5).

5 Conclusion

Detailed taxonomic and quantitative analyses of benthic foraminifera from ODP Site 752 (Broken Ridge) revealed no evidence of oxygen depletion in the upper intermediate waters of the southeastern Indian Ocean during the LMBB. Instead, the new evidence presented here suggests that oxic conditions persisted at intermediate depths in the last 9 Myr at Broken Ridge. We interpret these findings as indicating that the Indian Ocean OMZ did not reach Broken Ridge during the LMBB. Rather, we propose that modern-style TL significantly influenced benthic ecosystems at Broken Ridge since its onset in the Late Miocene (Figure 5). The benthic foraminifera distribution observed here is likely linked to the vigor of bottom water currents and the supply of intermediate-depth waters. Thus, we propose a new mechanistic model in which high-intensity TL limits the expansion of the OMZ in the southeastern intermediate-depth Indian Ocean.

Tasman Leakage is characterized by a bottleneck configuration south of Australia, with the Australian continent to the north and the Antarctic frontal system to the south. The intensity of TL and inter-basin exchange through this pathway from the Pacific

to the Indian Ocean is shaped by the interplay between tectonic configuration and the latitudinal position of climate belts. During the LMBB (Figures 5C,D), global climate was warm enough to keep the Antarctic frontal systems far south of southern Australia, enabling intense TL flow (Christensen et al., 2021; Lyu et al., 2023). This flow of TL waters prevented the expansion of oxygen-poor waters from the northern Indian Ocean into the southeastern Indian Ocean at the same depth.

While we interpret this TL-driven mechanism as the most plausible explanation for sustained oxygenation, we recognize that this conclusion is based on indirect evidence from benthic assemblages, sedimentological trends, and geochemical proxies. Future studies using isotopic water mass tracers will be essential to confirm the extent and timing of TL's influence on intermediate water masses in the Indian Ocean. That being said, our interpretation is supported by the alignment of benthic faunal shifts, geochemical evidence, and sedimentary patterns with known TL intensification. We therefore conclude that the Early Pliocene represented an optimal Earth System configuration for maximizing TL intensity—shaping benthic ecological conditions at ODP Site 752 and buffering this site from the OMZ expansion observed farther north in the Indian Ocean.

Data availability statement

Benthic foraminiferal row counts, microhabitat, oxygen index, and grouped species can be accessed via the PANGAEA data repository, <https://doi.pangaea.de/10.1594/PANGAEA.967492>, and are available as [Supplementary Materials](#).

Author contributions

JL: Data curation, Formal Analysis, Investigation, Software, Visualization, Writing – original draft, Writing – review and editing. SBM: Formal Analysis, Investigation, Writing – original draft, Writing – review and editing. GA: Investigation, Supervision, Writing – original draft, Writing – review and editing. OMB: Investigation, Supervision, Writing – original draft, Writing – review and editing. A-CS: Methodology, Software, Writing – original draft, Writing – review and editing. AVDG: Validation, Writing – review and editing. DDV: Conceptualization, Data curation, Formal Analysis, Funding acquisition, Investigation, Methodology, Project administration, Software, Supervision, Visualization, Writing – original draft, Writing – review and editing.

Funding

The author(s) declare that financial support was received for the research and/or publication of this article. The German Research Foundation (DFG) provided funding through Project 446900747 (VL96/3-1). A-C. The work contributes towards the Austrian Science Fund (FWF) grant P 36046-N awarded to GA. AVDG received financial support from the Alexander von Humboldt Foundation. A-CS was supported by a grant from Labex OSUG (Investissements

d'avenir – ANR10 LABX56). This study was conducted under the Repository Core Re-Discovery Program (ReC23-01), a collaborative program between Kochi Core Center and J-DESC.

Acknowledgments

This research used samples provided by the International Ocean Discovery Program (IODP) and the Ocean Drilling Program (ODP). We thank all scientific participants and crew of ODP Leg 121.

Conflict of interest

The authors declare that the research was conducted in the absence of any commercial or financial relationships that could be construed as a potential conflict of interest.

Generative AI statement

The author(s) declare that Generative AI was used in the creation of this manuscript. Generative AI was used to improve phrasing and grammar.

References

- Auer, G., Bialik, O. M., Antoulas, M. E., Vogt-Vincent, N., and Piller, W. E. (2023). Biotic response of plankton communities to Middle to Late Miocene monsoon wind and nutrient flux changes in the Oman margin upwelling zone. *Clim. Past.* 19 (11), 2313–2340. doi:10.5194/cp-19-2313-2023
- Berggren, W. A., Kent, D. V., Flynn, J. J., and Van Couvering, J. A. (1985). Cenozoic geochronology. *GSA Bull.* 96 (11), 1407–1418. doi:10.1130/0016-7606(1985)96<1407:cg>2.0.co;2
- Bialik, O. M., Auer, G., Ogawa, N. O., Kroon, D., Waldmann, N. D., and Ohkouchi, N. (2020). Monsoons, upwelling, and the Deoxygenation of the Northwestern Indian ocean in response to Middle to late Miocene global climatic shifts. *Paleoceanogr. Paleoclimatology* 35, 1–17. doi:10.1029/2019PA003762
- Bolli, H. M., Beckmann, J.-P., and Saunders, J. B. (1994). *Benthic foraminiferal biostratigraphy of the south Caribbean region*. Cambridge University Press.
- Bray, J. R., and Curtis, J. T. (1957). An Ordination of the Upland forest communities of southern Wisconsin. *Ecol. Monogr.* 27 (4), 325–349. doi:10.2307/1942268
- Christensen, B. A., De Vleeschouwer, D., Henderiks, J., Groeneveld, J., Auer, G., Drury, A. J., et al. (2021). Late Miocene onset of Tasman Leakage and southern Hemisphere Supergyre Ushers in near-modern circulation. *Geophys. Res. Lett.* 48 (18), e2021GL095036. doi:10.1029/2021GL095036
- Dickens, G. R., and Owen, R. M. (1994). Late Miocene-early Pliocene manganese redirection in the central Indian ocean: expansion of the intermediate water oxygen minimum zone. *Paleoceanography* 9 (1), 169–181. doi:10.1029/93PA02699
- Dickens, G. R., and Owen, R. M. (1999). The latest Miocene-early Pliocene biogenic bloom: a revised Indian ocean perspective. *Mar. Geol.* 161 (1), 75–91. doi:10.1016/S0025-3227(99)00057-2
- Diester-Haass, L., Meyers, P. A., and Vidal, L. (2002). The late Miocene onset of high productivity in the Benguela Current upwelling system as part of a global pattern. *Mar. Geol.* 180 (1), 87–103. doi:10.1016/S0025-3227(01)00207-9
- Driscoll, N. W., Weissel, J. K., Karner, G. D., and Mountain, G. S. (1991). Stratigraphic response of a carbonate Platform to relative sea level changes: Broken Ridge, Southeast Indian ocean 1. *AAPG Bull.* 75 (4), 808–831. doi:10.1306/0c9b285d-1710-11d7-8645000102c1865d
- Fisher, R. A., Corbet, A. S., and Williams, C. B. (1943). The relation between the number of species and the number of individuals in a random sample of an Animal Population. *J. Animal Ecol.* 12 (1), 42–58. doi:10.2307/1411
- Gastaldello, M. E., Agnini, C., Westerhold, T., Drury, A. J., Sutherland, R., Drake, M. K., et al. (2023). The late miocene-early Pliocene biogenic bloom: an integrated study in the tasman sea. *Paleoceanogr. Paleoclimatology* 38 (4), e2022PA004565. doi:10.1029/2022PA004565
- Geslin, E., Heinz, P., Jorissen, F., and Hemleben, C. (2004). Migratory responses of deep-sea benthic foraminifera to variable oxygen conditions: laboratory investigations. *Mar. Micropaleontol.* 53 (3), 227–243. doi:10.1016/j.marmicro.2004.05.010
- Glock, N. (2023). Benthic foraminifera and gromiids from oxygen-depleted environments – survival strategies, biogeochemistry and trophic interactions. *Biogeosciences* 20 (16), 3423–3447. doi:10.5194/bg-20-3423-2023
- Gupta, A. K., Singh, R. K., and Verma, S. (2013). Deep-sea palaeoceanographic evolution of the eastern Indian Ocean during the late Oligocene–Pleistocene: species diversity trends in benthic foraminifera. *Curr. Sci.* 104 (7), 904–910.
- Hammer, Ø., and Harper, D. A. (2001). Past: paleontological statistics software package for education and data analysis. *Palaeontol. Electron.* 4 (1), 1.
- Hermoyian, C. S., and Owen, R. M. (2001). Late miocene-early Pliocene biogenic bloom: evidence from low-productivity regions of the Indian and atlantic oceans. *Paleoceanography* 16 (1), 95–100. doi:10.1029/2000PA000501
- Holbourn, A., Henderson, A. S., and MacLeod, N. (2013). *Atlas of benthic foraminifera*. John Wiley & Sons.
- House, M. A., Rea, D. K., and Janecek, T. R. (1991). “Grain-size record of Ocean current winnowing in oligocene to pleistocene ooze, Broken Ridge, southeastern Indian ocean,” in *Proceedings of the OceanDrilling program. Scientific results*. J. K. Weissel, J. Peirce, T. E., J. Alt, et al. (College Station, Texas, USA: Ocean Drilling Program), 211–218.
- Jensen, M. M., Lam, P., Revsbech, N. P., Nagel, B., Gaye, B., Jetten, M. S. M., et al. (2011). Intensive nitrogen loss over the Omani Shelf due to anammox coupled with dissimilatory nitrite reduction to ammonium. *ISME J.* 5 (10), 1660–1670. doi:10.1038/ismej.2011.44
- Jorissen, F. J., de Stigter, H. C., and Widmark, J. G. V. (1995). A conceptual model explaining benthic foraminiferal microhabitats. *Mar. Micropaleontol.* 26 (1), 3–15. doi:10.1016/0377-8398(95)00047-X
- Kaiho, K. (1994). Benthic foraminiferal dissolved-oxygen index and dissolved-oxygen levels in the modern ocean. *Geology* 22 (8), 719–722. doi:10.1130/0091-7613(1994)022<0719:bfdioa>2.3.co;2
- Karatsolis, B. T., Lougheed, B. C., De Vleeschouwer, D., and Henderiks, J. (2022). Abrupt conclusion of the late Miocene-early Pliocene biogenic bloom at 4.6–4.4 Ma. *Nat. Commun.* 13 (1), 353. doi:10.1038/s41467-021-27784-6

Publisher's note

All claims expressed in this article are solely those of the authors and do not necessarily represent those of their affiliated organizations, or those of the publisher, the editors and the reviewers. Any product that may be evaluated in this article, or claim that may be made by its manufacturer, is not guaranteed or endorsed by the publisher.

Supplementary material

The Supplementary Material for this article can be found online at: <https://www.frontiersin.org/articles/10.3389/feart.2025.1528487/full#supplementary-material>.

SUPPLEMENTARY FIGURE S1

Cibicides wuellerstorfi. (a–c) from ODP Hole 752A, 2H-2,100–102 cm. (a) umbilical view; (b) edge view; (c) spiral view. (d–f) from ODP Hole 752A, 2H-1, 4–6 cm. (d) umbilical view; (e) edge view; (f) spiral view. (g–i) from ODP Hole 752A, 2H-1, 4–6 cm. (g) umbilical view; (h) edge view; (i) spiral view.

SUPPLEMENTARY FIGURE S2

Hanzawaia boueana. (a–c) from ODP Hole 752A, 3H-3,10–12 cm. (a) umbilical view; (b) edge view; (c) spiral view. (d–f) from ODP Hole 752A, 2H-4,118–120cm. (d) umbilical view; (e) edge view; (f) spiral view. (g–i) from ODP Hole 752A, 2H-4,118–120cm. (g) umbilical view; (h) edge view; (i) spiral view.

- Kouwenhoven, T. J. (2000). *Survival under stress: benthic foraminiferal patterns and Cenozoic biotic crises*. Utrecht, Netherlands: Faculteit Aardwetenschappen.
- Kraal, P., Slomp, C. P., Reed, D. C., Reichart, G. J., and Poulton, S. W. (2012). Sedimentary phosphorus and iron cycling in and below the oxygen minimum zone of the northern Arabian Sea. *Biogeosciences* 9 (7), 2603–2624. doi:10.5194/bg-9-2603-2012
- Kranner, M., Harzhauser, M., Beer, C., Auer, G., and Piller, W. E. (2022). Calculating dissolved marine oxygen values based on an enhanced Benthic Foraminifera Oxygen Index. *Sci. Rep.* 12 (1), 1376. doi:10.1038/s41598-022-05295-8
- Lewis, B. L., and Luther Iii, G. W. (2000). Processes controlling the distribution and cycling of manganese in the oxygen minimum zone of the Arabian Sea. *Deep Sea Res. Part II Top. Stud. Oceanogr.* 47 (7), 1541–1561. doi:10.1016/S0967-0645(99)00153-8
- Linke, P., and Lutze, G. F. (1993). Microhabitat preferences of benthic foraminifera—a static concept or a dynamic adaptation to optimize food acquisition? *Mar. Micropaleontol.* 20 (3), 215–234. doi:10.1016/0377-8398(93)90034-U
- Loeblich Jr, A. R., and Tappan, H. (2015). *Foraminiferal genera and their classification*. Springer.
- Lyle, M., Drury, A. J., Tian, J., Wilkens, R., and Westerhold, T. (2019). Late Miocene to Holocene high-resolution eastern equatorial Pacific carbonate records: stratigraphy linked by dissolution and paleoproductivity. *Clim. Past* 15 (5), 1715–1739. doi:10.5194/cp-15-1715-2019
- Lyu, J., Auer, G., Bialik, O. M., Christensen, B., Yamaoka, R., and De Vleeschouwer, D. (2023). Astronomically-paced changes in paleoproductivity, winnowing, and mineral flux over Broken Ridge (Indian ocean) since the early Miocene. *Paleoceanogr. Paleoclimatology* 38 (12), e2023PA004761. doi:10.1029/2023PA004761
- Mutter, J. C., and Cande, S. C. (1983). The early opening between Broken Ridge and Kerguelen Plateau. *Earth Planet. Sci. Lett.* 65 (2), 369–376. doi:10.1016/0012-821X(83)90174-7
- Peirce, J. W., Weissel, J. K., Taylor, E., Dehn, J., Driscoll, N., Farrell, J., et al. (1989). “Site 752,” in Proceedings of the Ocean Drilling Program (College Station, TX, United States: Texas A & M University, Ocean Drilling Program), 111–169. *Initial Reports*.
- Pillot, Q., Suchéras-Marx, B., Sarr, A. C., Bolton, C. T., and Donnadieu, Y. (2023). A global reassessment of the spatial and temporal expression of the late Miocene biogenic bloom. *Paleoceanogr. Paleoclimatology* 38 (3), e2022PA004564. doi:10.1029/2022PA004564
- Piotrowski, A. M., Banakar, V. K., Scrivner, A. E., Elderfield, H., Galy, A., and Dennis, A. (2009). Indian Ocean circulation and productivity during the last glacial cycle. *Earth Planet. Sci. Lett.* 285 (1), 179–189. doi:10.1016/j.epsl.2009.06.007
- Raddatz, J., Beisel, E., Butzin, M., Schröder-Ritzrau, A., Betzler, C., Friedrich, R., et al. (2023). Variable ventilation ages in the equatorial Indian Ocean thermocline during the LGM. *Sci. Rep.* 13 (1), 11355. doi:10.1038/s41598-023-38388-z
- Ridha, D., Boomer, I., and Edgar, K. M. (2019). Latest oligocene to earliest Pliocene deep-sea benthic foraminifera from Ocean Drilling program (ODP) sites 752, 1168 and 1139, southern Indian ocean. *J. Micropaleontol.* 38 (2), 189–229. doi:10.5194/jm-38-189-2019
- Sarr, A. C., Donnadieu, Y., Laugié, M., Ladant, J. B., Suchéras-Marx, B., and Raison, F. (2022). Ventilation changes drive orbital-scale deoxygenation trends in the late cretaceous ocean. *Geophys. Res. Lett.* 49 (19), e2022GL099830. doi:10.1029/2022GL099830
- Singh, R. K., Gupta, A. K., and Das, M. (2012). Paleooceanographic significance of deep-sea benthic foraminiferal species diversity at southeastern Indian Ocean Hole 752A during the Neogene. *Palaeoogeogr. Palaoclimatol. Palaeoecol.* 361–362, 94–103. doi:10.1016/j.palaeo.2012.08.008
- Slater, R., and Kroopnick, P. (1984). Controls of dissolved oxygen distribution and organic carbon deposition in the Arabian Sea. *Geol. Oceanogr. Arabian Sea Coast. Pak.*, 305–313.
- Sokal, R. R. (1965). Statistical methods in systematics. *Biol. Rev.* 40 (3), 337–389. doi:10.1111/j.1469-185x.1965.tb00806.x
- Sokal, R. R., and Rohlf, F. J. (1962). The comparison of dendrograms by objective methods. *Taxon* 11 (2), 33–40. doi:10.2307/1217208
- Struve, T., Wilson, D. J., Hines, S. K. V., Adkins, J. F., and van de Fliedert, T. (2022). A deep Tasman outflow of Pacific waters during the last glacial period. *Nat. Commun.* 13 (1), 3763. doi:10.1038/s41467-022-31116-7
- Sutherland, R., Dos Santos, Z., Agnini, C., Alegret, L., Lam, A. R., Westerhold, T., et al. (2022). Neogene mass accumulation rate of carbonate sediment across Northern Zealandia, Tasman Sea, Southwest Pacific. *Paleoceanogr. Paleoclimatology* 37 (2), e2021PA004294. doi:10.1029/2021PA004294
- van der Zwaan, G. J., Jorissen, F. J., and de Stigter, H. C. (1990). The depth dependency of planktonic/benthic foraminiferal ratios: constraints and applications. *Mar. Geol.* 95 (1), 1–16. doi:10.1016/0025-3227(90)90016-D
- Van Morkhoven, F. (1986). Cenozoic cosmopolitan deep-water benthic foraminifera. *Bulletin Centres Rech. Exploration-Production Elf-Aquitaine Mémoire* 11.
- Wyrтки, K., Bennett, E. B., and Rochford, D. J. (1971). *Oceanographic atlas of the international Indian Ocean expedition*. Washington DC: National Science Foundation.
- You, Y. (2000). Implications of the deep circulation and ventilation of the Indian ocean on the renewal mechanism of north Atlantic deep water. *J. Geophys. Res. Oceans* 105 (C10), 23895–23926. doi:10.1029/2000JC900105